Materials Science and Engineering C 29 (2009) 1835–1841

Contents lists available at ScienceDirect

Materials Science and Engineering C

journal homepage: www.elsevier.com/locate/msec

Polyurethane unimorph bender microfabricated with Pressure Assisted Microsyringe (PAM) for biomedical applications

G. Tartarisco [a], G. Gallone [a,b], F. Carpi [a], G. Vozzi [a,b,*]

[a] Interdepartmental Research Center "E. Piaggio", Faculty of Engineering, University of Pisa, Via Diotisalvi,2, 56126 Pisa, Italy
[b] Department of Chemical Engineering Industrial Chemistry and Materials Science (DICCISM), Faculty of Engineering, University of Pisa, Via Diotisalvi,2, 56126 Pisa, Italy

ARTICLE INFO

Article history:
Received 23 July 2008
Received in revised form 27 January 2009
Accepted 18 February 2009
Available online 6 March 2009

Keywords:
Microfabrication
Polyurethane
Carbon black
Actuator
PAM system

ABSTRACT

This paper describes a new microfabrication technique for bender-type electromechanical actuators made of an elastomeric electroactive polymer. The technique is based on a computer-controlled deposition of the active material with a microsyringe. The paper describes the developed microfabrication system and proposes a simple deposition model. The realization of solid-state unimorph bender actuators made of polyurethane as electrolyte and a mixture of carbon black and polyurethane as electrodes is presented. Prototype actuators fabricated both with the new technique were driven with electrical field of 100 V/μm and showed bending angles higher than 30°. In this way, we have demonstrated that it is possible to fabricate polyurethane based microactuators using a polyurethane/carbon black composite such as device.

1. Introduction

The continuous progress in the field of advanced robotics and bioengineering has pushed the development of new methodologies for the realisation of small-scale electromechanical actuation devices, able to convert electrical power into mechanical energy so that to transfer motion to loads. In the last years, a considerable amount of research has been carried out on electroactive polymers (EAP), particularly about elastomeric polymers such as polyurethane and silicone [1]. An analysis of the literature has shown the presence of miniaturized actuators realized with piezoelectric EAP and ionic EAP [2,3]; also, many reviews have been focused on electroactive polymers concerning either the mimicking of natural muscles [4] or specific applications including naval [5,6], space [7], medical and other biomimetic technologies [8,9]. Ionic EAPs, including electro-chemo-mechanical conducting polymers, ionic polymer metal composites, and mechano-chemical polymers/gels, are largely affected by low response speeds (strain rates) and extents, with the exception of the latters, and limited actuation stresses, owing to their predominantly diffusion-dependent actuation mechanisms [8]. While capable of higher actuation speeds, electronic EAPs such as electrostrictive and piezoelectric polymers but even lesser achievable strains [8]. Dielectric elastomers (DEs), on the other hand, present many advantages in terms of active strains and stresses, speed of response, reliability, durability and efficiency, as well as easiness of processing [10–20]. It is reported that DEs actuators can achieve strains of the order of 10–100% and can develop stresses up to 1 MPa [14]. As a fact, DEs measure up very well when compared to natural muscles in terms of typical stress and strain, energy and power densities, peak strain rate, response speed and efficiency [8]. In the light of their biomimetic potential and following the growing interest in their technological development, DEs were selected for detailed exploration with regards to biomedical applications.

The principle of operation of any dielectric elastomer actuator can be easily described in relation to the elementary actuating configuration, consisting of a parallel plate deformable capacitor: the application of a suitable electrical tension to a couple of compliant electrodes located on the main surfaces of a thin DE film, results in a compression of the sandwiched elastomer along its thickness, while related orthogonal elongations (transverse strain) occur [11,13,15]. Thus, the actuation process originates simply as the consequence of the so-called Maxwell stress, arising from the electrostatic attraction between the two oppositely charged electrodes. However, despite the high-level actuating performances enabled by this kind of materials, their extensive use is presently limited by the required high driving electric fields, typically of 10–100 V/μm [10–20].

A possible configuration realised with these materials is represented by the unimorph bender actuator, which consists of two films of active material coupled to the sides of a passive supporting layer: the polyurethane. A typical fabrication route for such kind of actuators is based on casting the polymer solution in mini-molds [21]. Recently, more innovative methods such as ink-jet printing [22–24], soft lithography [13–28] and deposition via either controlled-volume or pneumatic microsyringes have been proposed [29].

* Corresponding author. Interdepartmental Research Center "E. Piaggio", Faculty of Engineering, University of Pisa, Via Diotisalvi,2, 56126 Pisa, Italy.
E-mail address: g.vozzi@ing.unipi.it (G. Vozzi).

0928-4931/$ – see front matter © 2009 Elsevier B.V. All rights reserved.
doi:10.1016/j.msec.2009.02.017

In this paper we present a microfabrication process for bender actuators by means of a pressure-controlled microsyringe (PAM) mounted on a computer controlled three-axis micropositioner. The system was used for the fabrication of a *unimorph bender* actuator composed of two external layers made of a carbon black filled polyurethane, which worked as electrodes, and an inner layer made of neat polyurethane.

2. Materials

2.1. Dielectric elastomer

The EAP used in this work was a commercial polyurethane elastomer, available as a bicomponent A and B (Polytek 74-20, Polytek, USA). According to the manufacturer specifications, the material was processed by adding curing agent B to component A at a B:A = 2:1 weight ratio.

2.2. Electrodes

Compliant electrodes to be coupled to the dielectric elastomer were made by a composite approach: the same polyurethane matrix was loaded by fine carbon black (CB) powder in order to obtain a conductive elastomer with high compatibility with the DE in terms of both surface adhesion and elastic modulus. However, carbon black grains normally aggregates to form a kind of "unit base" [30]; this gives rise to a technological issue when the CB has to be extruded through very narrow needles since these may end up obstructed by larger particles. Thus, a dispersant EFKA 4010 (Ciba, Italy) was added during the loading of polyurethane with carbon black, in order to avoid the formation of agglomerates and obtain an optimal extrusion through the needle of the microfabrication system. The dispersant was added to a 3.3 wt/vol.% solution in trichloroethylene of component A of Polytek 74 in a quantity pair to 60% weight of CB. The obtained CB and polyurethane suspension was stirred for half hour with a sonicator (Vibra-cell, Sonics, USA). Thereafter, a proper amount (see Section 2.1) of component B was added and the whole suspension was stirred for further 5 min before it was extruded by the PAM system to form the electrodes of the bender.

3. Methods

3.1. Microfabrication technique

Planar bending actuators were fabricated by means of a microfabrication technique developed in our laboratory. The deposition system consisted of a 10 ml stainless steel syringe with a 20 mm-long glass capillary needle as the tip. A home-built vertical puller was used to pull the tips, which were prepared from soda glass hematocrit capillaries (Globe Scientific, Paramus, NJ) with an outer diameter of 1.5 mm and an inner diameter of 1.15 mm. Each capillary was pulled under the same conditions and the resulting internal diameter of the obtained tips was 20 ± 2 μm. The needle was connected to the syringe barrel and hold in place by a small O-ring. The syringe had no plunger and was driven by filtered compressed air supplied at pressures ranging between 5 and 300 mmHg; it was attached to the vertical *z* axis of a three-axis stepper-motor micropositioning system capable of 0.1 μm resolutions. A planar substrate was fixed on the horizontal *x*–*y* plane of the micropositioner and was made to move under the syringe during deposition. When a pressure was applied to the syringe, tiny amounts of polymer oozed out through the tip. Purposely written software allowed almost any type of structure to be deposited in sequential layers by simply translating a black and white jpeg or bitmap image into a sequential list of linear coordinates which were then used to drive the motors toward the right *x* and *y* position. For example, in previous works we succeeded in microfabricating spirals, square, hexagonal and octagonal grids as well as fractal branches [29–31].

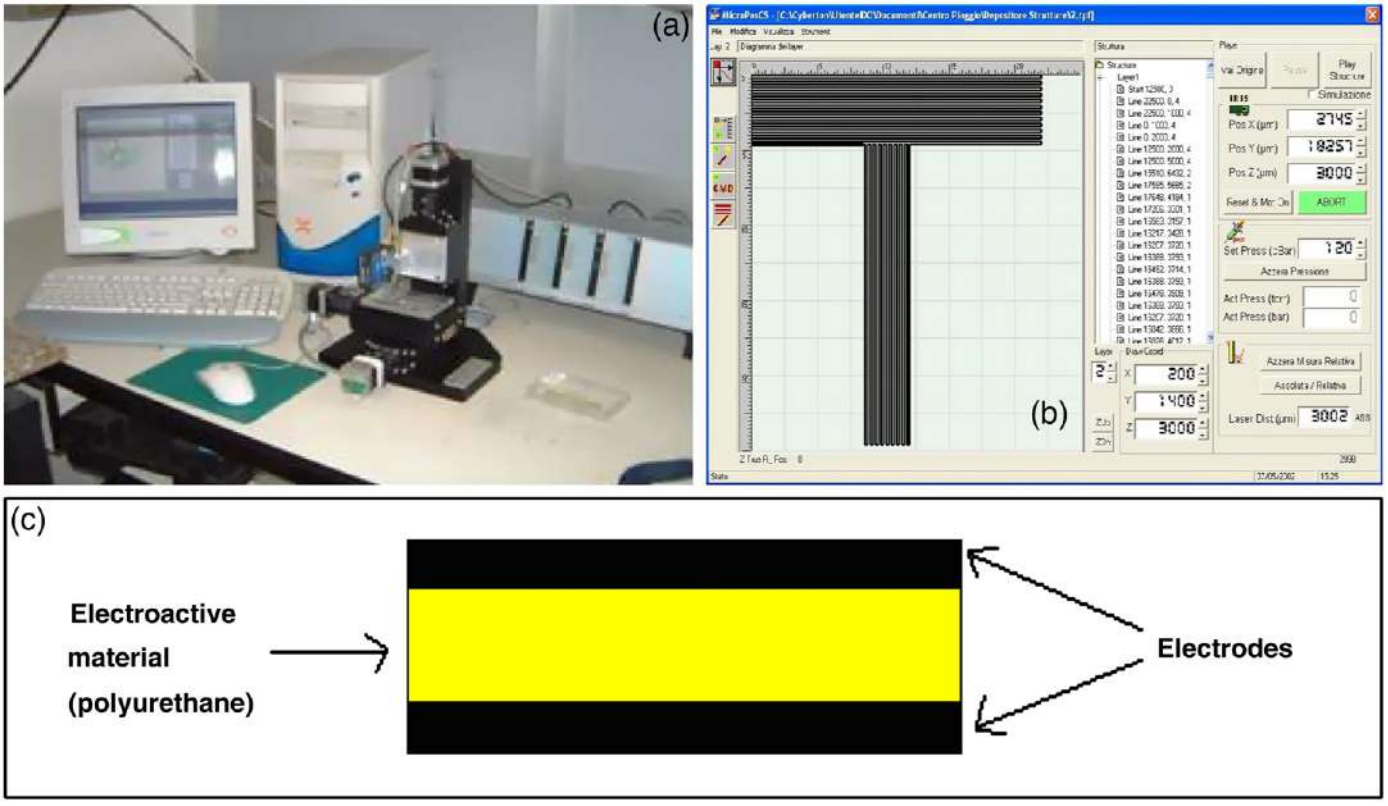

Fig. 1. (a) The PAM system. (b) CAD design of bender realised. (c) Scheme of the bimorph bender actuator realised in this work.

Fig. 1a presents a picture of the complete PAM setup, while in Fig. 1b it is visible the CAD drawing of the realised bender. The technique described above was used to fabricate unimorph bender actuators, where two electrode layers sandwich the elastomeric polyurethane layer, as shown in Fig. 1c.

3.2. Deposition model

Complex models such as those used in dynamic wetting systems can be used to predict the line width and height of the patterns deposited. Such models use the dynamic contact angle, which requires flow visualization techniques to be measured, to parameterize the equilibrium configuration of a liquid in a coating system [32]. As a first approximation, we developed a simple fluid-dynamic model that enables the prediction of the width and height of the patterns. The model is focused on the conditions at the tip of the needle, i.e. exactly the point where the polymer exits.

We assume that there is a simple geometry at the tip, and that the properties of the polymer solution are not sensibly affected by solvent evaporation soon after its extrusion [29]. As shown in Fig. 2, the forces acting at the tip where the fluid is expelled are:

- the driving pressure, P, and the weight of the polymer in the syringe barrel (mg);
- the vapour pressure of the solvent, P^*;
- the surface tension at the interface between polymer solution and air, γ
- the dynamic friction between fluid and glass, which is a function of the viscosity of the solution, μ.

If the balance of all forces and energies at the tip of the syringe is considered, a multivariable system of equations with an infinite number of solutions should be solved in order to predict the width and height of the patterns. To simplify the model, we assume that the driving pressure P, is the dominant force in such a system, while the other forces can be neglected. Hence, the flow of the polymer from the needle Q is:

$$Q = \frac{dV}{dt} \tag{1}$$

where V is the volume of polymer deposited and t is the time. Under the assumption that the extrusion process may be assimilated to the streamlined flow of a viscous Newtonian fluid, the Poiseulle's equation provides the flow inside the capillary:

$$Q = \frac{\pi R_s^4}{8\mu}\frac{dp}{dz} \tag{2}$$

where R_s is the internal radius of the needle tip, dp/dz the total applied pressure gradient and μ the viscosity of the polymer. On the other hand, the lines profiles can be approximated to elliptical segments and, given their high aspect ratio (line width to height), the product of height and width can be used to estimate the cross-sectional area of the deposited structures. Thus, we can approximate the volume V of the fluid extruded in a time t to be:

$$V = ahl \tag{3}$$

where a is the line width, h is the height of the polymer pattern and l is the length of polymer deposited in a time t, hence $v_o = l/t$.

Substituting Eqs. (3) and (2) in Eq. (1), the line width a can be written as:

$$a = \frac{\pi R_s^4}{8\mu v_0 h}\frac{dp}{dz} \tag{4}$$

In order to let the fluid to flow out of the tip, a certain critical pressure, P_{crit}, proportional to the viscosity of the solution, must be applied. In fact, at pressures below such threshold the frictional forces are greater than the driving one and deposition cannot occur. The pressure gradient is negligible throughout the most part of the syringe, and effectively it raises and reaches its maximum just in the tapered region of the tip. In this model, dp/dz has been approximated to $(P+P_{crit})/h_z$, being $P+P_{crit}$ the applied driving pressure, h_z the length of the tapered zone in the capillary and having neglected the atmospheric pressure at the exit. Eq. (4) can then be expressed as:

$$a = \frac{\pi R_s}{8\mu v_0 h}\frac{(P + P_{crit})}{h_z} \tag{5}$$

For a given profile aspect ratio, the model can be used to predict line width, a, as a function of applied air pressure P, motor velocity, v_o and polymer viscosity μ. If the profile of the pattern is to be determined, the width to height ratio of the deposited lines can be estimated by recursive methods from an experimental plot of driving pressure against line width, assuming a rectangular profile. By means of Eq. (5), the experimental pressure was fitted to the deposited polymer line width data.

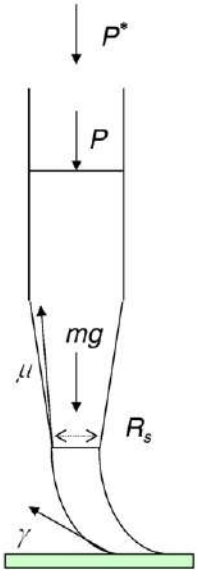

Fig. 2. Scheme of forces acting in PAM system.

3.3. Stress–strain testing

Realization of stress–strain tests allowed measuring the various Young's modulus for the following depositions:

- Polyurethane film;
- Mixture of carbon black and polyurethane;
- Polyurethane film in with electrodes on both sides;

The mechanical properties of the samples were measured by means of an isotonic transducer (model 7006, UGO Basile Biological Research Apparatus, Italy), capable of an applied force resolution of 1 mN. Two small strips of transparent acetate (20×5 mm^2) were glued to either side of one end of the sample and a small hole was pierced in the transparency in order to attach the sample to the transducer lever. The other end was held firmly by a small clamp. The applied force acted along the direction of maximal length of the structures.

During the stress–strain tests, the applied weights were changed every 3 min, and then the Young's modulus of each structure was measured as the slope at null strain in the resulting curve. The

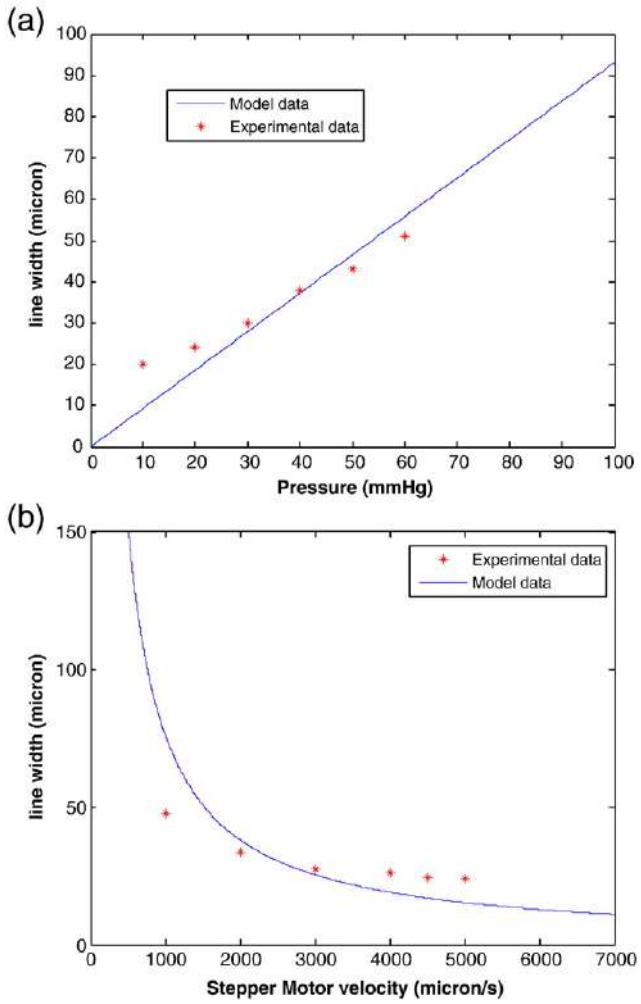

Fig. 3. Experimental and modelled tracks widths as a function of: (a) applied pressure (at a stepper motor speed of 2500 μm/s), and (b) motor speed (at an applied pressure of 30 mmHg).

acquisition has executed through a software purposely developed (Biolab 3,7, Italy).

3.4. Actuator testing

Preliminary bending tests were carried out on prototype unimorph strips fabricated with the described technique. A standard characterization method was used for such a purpose. In particular, the active driving of the DE actuators was obtained by applying a controlled difference of potential to the opposite electrodes of each strip. Stimulation was generated by using a potentiostat (model 273, EG&G Princeton Applied Research, USA) to obtain driving electric field with amplitudes ranging between −100 and +100 V/μm. Sample actuators were arranged in a vertical position, constrained only at their upper part while the rest of their body was left free, and were operated in air. As the supplied electrical tension was varied within the considered range, the displacement of the electrically stimulated DE actuator was measured by means of an optical sensor (Opto NCDT, model ILD1400-10, UK), having a nominal resolution of 1 μm.

4. Results and discussion

4.1. Fabrication of the bender

The PAM system permitted the realization of all different types of layers required by the fabrication of unimorph bender actuators. Data related to the deposition of the polyurethane layer and mixed polyurethane and CB electrode layers are separately presented below.

Initially a structure with a serpentine topology was realised, and for each line was varied the pressure for a fixed velocity, or was varied the velocity for a fixed pressure. The line width of the calibration structures was measured using an optical microscope with a 10× objective. Each line of the pattern was measured at three extreme points and then for each group of lines realised with same pressure or velocity the mean value and standard deviation was calculated. Standard deviations were typically around 10%.

Fig. 3a and b shows the line width for extruded polyurethane as a function of pressure and velocity respectively. As expected, the line width increased with increasing pressure and decreased with increasing velocity. The line width trend showed to be almost linear and in agreement with the model described above, at least for pressure higher than 30 mmHg. Experimental deviation from the model at lower pressure might be ascribed to possible pressure drops somewhere between the pressure sensor and the extrusion tip.

Samples with line widths between 20 and 60 μm, for pressures comprised between 10 and 60 mmHg, could be realised by increasing motor speed (5500 μm/s) and decreasing the diameter of the syringe tip down to 1 μm. A great degree of control over sample lateral features was obtained using PAM. For example, by changing the deposition pressure from 10 to 60 mmHg, it was possible to obtain lateral feature ranging from 20 μm to 60 μm. As far as fidelity is concerned, for linear trajectories the scaffold lateral dimensions were to within about 10% of those input into the design files. From the motor and driver specifications, we estimated that the motion in both

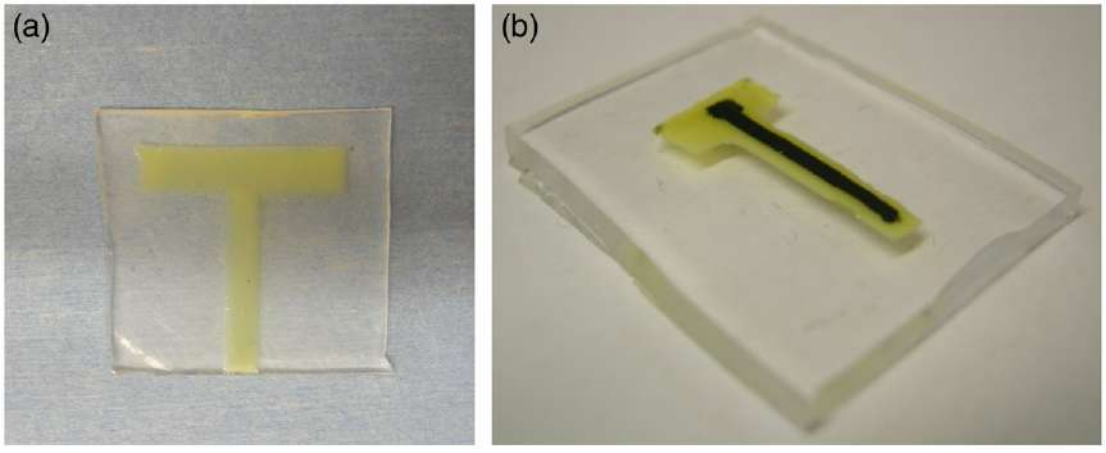

Fig. 4. A polyurethane dielectric layer deposited by PAM system (a), and a carbon black electrode layer deposited by PAM system above a polyurethane layer (b).

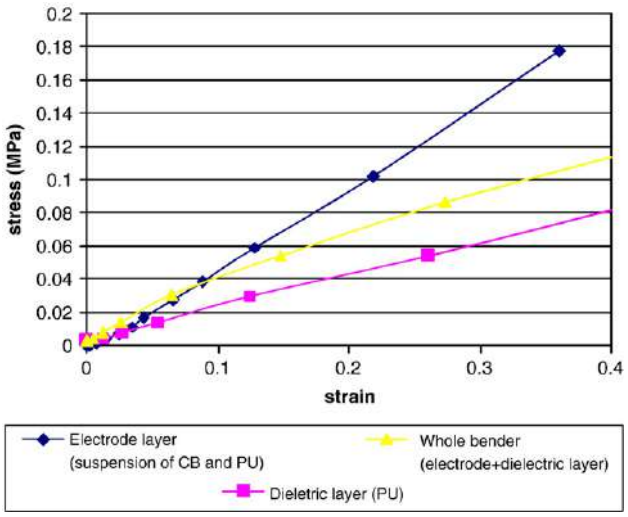

Fig. 5. Stress–strain curves for the dielectric layer (polyurethane), the electrode layer (polyurethane/carbon black composite) and for the assembled actuator.

x and *y* directions was able to attain constant velocity after the first 5 μm extruded from the rest. Of greater significance however, it was the fidelity of the system in areas where the motors had to accelerate or decelerate because of a change of direction in the design trajectory, as for example at the corners of a serpentine, where the deposited features were larger than the design file features. Therefore, the fidelity of the structure decreased with an increase in radius of curvature. Nevertheless a constant velocity and linear trajectory was achieved in our microfabrication system, thanks to a purposely developed algorithm, able to compensating the increase of line width in the change of direction trough a calibrated decrease of pressure extrusion. On the basis of the experimental graphs we chose the working parameters to obtain tracks approximately of 30–50 μm of width:

- deposition pressure: $P = 30$ mmHg;
- deposition speed: $v_{dep} = 2500$ μm/s.

Polyurethane was extruded on a silicone substrate, obtaining a strip 3 mm width, 2 cm length and with variable thicknesses between 150 and 200 μm, were obtained (Fig. 4a).

Subsequently, compliant electrodes made of a dispersion of carbon black in polyurethane were deposited on both surfaces of the strips (Fig. 4b). By this way a dielectric elastomer bender actuator was obtained.

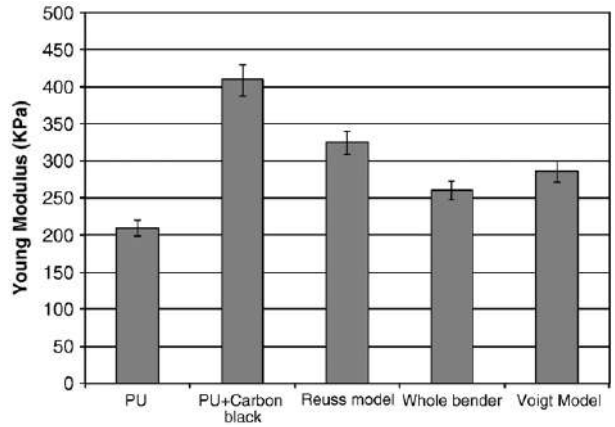

Fig. 6. Comparison of the Young's modulus values for the various materials and structures presented in this work and for two considered mechanical models (see text).

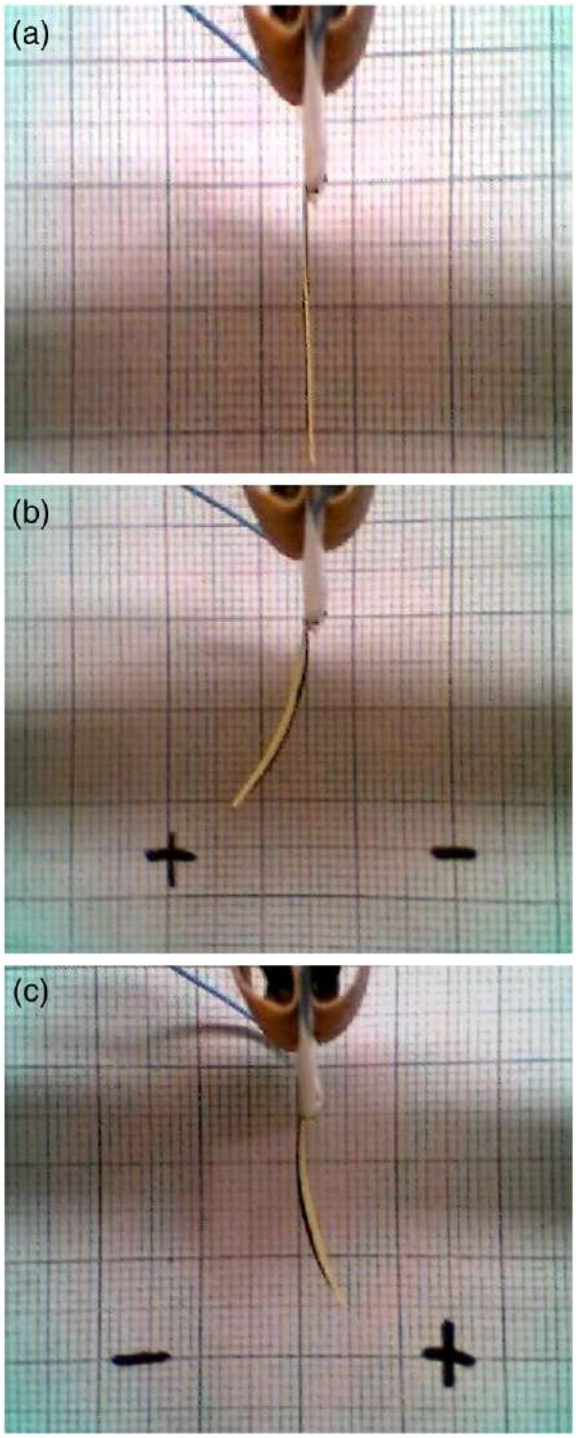

Fig. 7. Pictures of the actuator taken (a) during its stimulation by a voltage of +3000 V (positive bending), (b) at rest, (c) at an applied voltage of −3000 V (negative bending).

4.2. Stress–strain

Mechanical tests were performed on both samples of PU, PU/CB composites and on the whole bender. Fig. 5 shows the stress–strain behaviour of the three different systems. At first glance, it is evident that the stress–strain characteristics had the typical trend of an elastomeric material, moreover, addition of CB worsened the elastic properties of the polyurethane.

By assuming that the PU/CB coupled system may be assimilated to a composite material, the response can be compared to the prediction of mechanical models by Reuss or Voigt [33] (Fig. 6), where the elastic

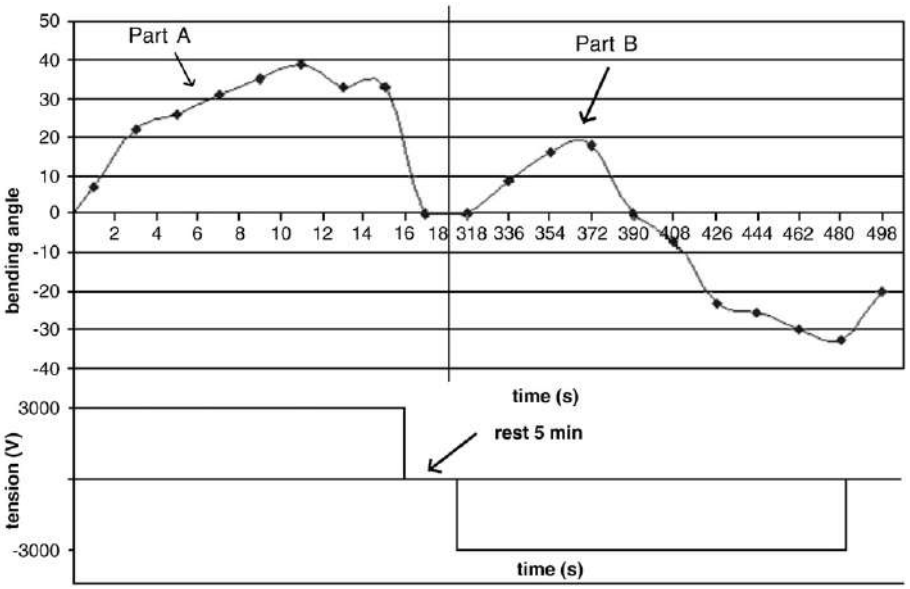

Fig. 8. Time behaviour of bending angle of the actuator during the voltage stimulation.

modulus is evaluated as a parallel or series composition of those of the pure material. The layer of PU/CB composite electrode presented an elastic modulus that could not be modelled by such simple assumptions; the whole bender, instead, showed a Young modulus value very close to that from Voigt model. This result confirmed that both the constituting phases worked effectively in isostrain configuration.

Anyway all the measured Young moduli resulted of the same order of magnitude, thus demonstrating that the deposition of such electrodes only minimally influences the rigidity of the polymer and does not hinder its flexibility.

4.3. Actuation

The realised bender showed an opposite bending during the positive and negative periods of the stimulation, with a maximum bending higher than 30°. Three pictures of the bender at rest (Fig. 7b) and in correspondence of opposite applied voltages (Fig. 7a–c) are visible in Fig. 7, while in Fig. 8, both the achieved bending angles and the applied signal are plotted as function of time.

A peculiar behaviour was observed in what concerns the switching capabilities of the bender. In fact, when the applied voltage was inverted, i.e. the polarity was changed from positive to negative, the bender initially had a flexion toward the previous "positive" bending direction before turning toward the expected negative angles values after few seconds. Such behaviour was observed even after letting a five minutes rest period at zero volts before a voltage sign switching. A possible explanation for this phenomenon can be formulated by supposing the presence, inside the bender, of positive and negative charged particles or segmental bodies with different diameter, mass and mobility one or both being capable of displacement (translation, rotation or tumbling) under the action of an electric field. Such charges could be represented by well defined individuals as, for example, pairs of ions and counter ions, or spread bodies, as oppositely charged distributions at the edges of existing dipoles. Thus, the voltage applied to the bender generates selective charge migration toward electrodes, which is not necessarily required to occur at a long range, as would be expected in simple dipolar reorientation. This would in any case result in a difference of elastic modules at the bender surfaces which, in response to the Maxwell stress contemporarily acting on the DE, causes its flexion by the same mechanism acting in bimorph benders. However, it is clear that in such a kind of system the differences in the rigidity of the opposite surfaces are not fixed *a priori*, as in usual bimorph benders, rather they are supposed to be induced by the same driving field and thus to be dependent from its polarity as well. Nevertheless, when the voltage polarity is switched, the response of our device shows a transient which should account for the mechanical relaxation that the system must undergo, presumably involving different time scales for different charge types. Thus, only when a complete redistribution of charges has taken place the bender can start to bend coherently with the new inverted voltage polarity. Instead, during the transient, the system maintains a sort of "fading memory" of its surfaces rigidities, so that any Maxwell stress applied at this moment to the device, whatever the driving tension polarity, will cause a bending in the previously memorized direction.

It must be pointed out that such description represents just an attempt to give a picture consistent with the observed behaviour and compatible with the nature of the involved materials. In effects, at the moment it is not supported (nor refuted) by any chemical analysis and a more accurate characterization would be required in order to confirm the validity of the proposed hypothesis. Anyway, such a study is beyond the scopes of this work, whose main goal was the fabrication of a DE actuator by using a PAM technique. The figure of merit of the fabricated bender is presented in Fig. 9, where it is clearly visible that the actuation properties of the device in terms of bending resulted to be regular and fairly symmetrical with respect to amplitude and sign of the applied potential.

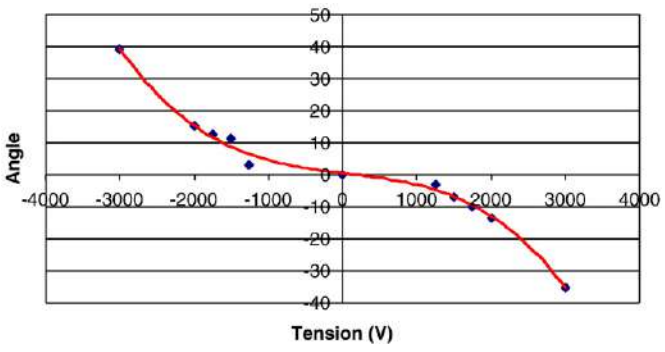

Fig. 9. Bending angle as function of the applied voltage.

5. Conclusions

We demonstrated that it is possible to fabricate polyurethane based microactuators by using a Pressure Assisted Microsyringe system.

The use of a polyurethane matrix mixed with carbon black and a suitable dispersant agent allowed obtaining suspensions with an optimal viscosity such that they could be processed with the PAM system. Such composite approach assured a perfect adhesion between conductive and electroactive layers and reduced the effect of stress shielding between different layers. A physical model of the microfabrication system was also proposed and it showed reasonable agreement with the experimental deposition data in the relevant pressure range. Bender prototypes were realised and stimulated in air by potential differences ranging between −3000 and +3000 V, showing bending angles higher than 30°.

At present, an extensive characterization of the electromechanical performances of bender actuators realized with this technique is being carried out in our laboratories. A full control of the edge roughness/waviness and the film thickness uniformity across the printed area is to be considered a key issue for the quality assessment of the product of this technology.

References

[1] Geoffrey M. Spinks, Gordon G. Wallace, Jie Ding, Dezhi Zhou, Binbin Xi, Timothy R. Scott, Van-Tan Truong, Proceedings of SPIE — The International Society for Optical Engineering, vol. 5051, 2003, p. 21.
[2] I. Krakovsky, T. Romijn, A. Posthuma de Boer, J. Appl. Phys. vol. 85 (1999) 628.
[3] T. Yamwong, A.M. Voice, G.R. Davies, J. Appl. Phys. vol. 91 (2002) 1472.
[4] Y. Bar-Cohen (Ed.), Electroactive polymer (EAP) Actuators as Artificial Muscles, SPIE Press, Washington, 2001.
[5] A. Vinogradov, J. Su, C. Jenkins, Y. Bar-Cohen, Symposium (Materials Research Society Symposium Proceedings, vol. 889, 2006, p. 51.
[6] J.D.W. Madden, N.A. Vandesteeg, P.A. Anquetil, P.G.A. Madden, A. Takshi, R.Z. Pytel, et al., IEEE J. Ocean Eng. 29 (2004) 706 Full Text via CrossRef | View Record in Scopus | Cited By in Scopus (83).
[7] Y. Bar-Cohen, Proceedings-2004 NASA/DoD Conference on Evolvable Hardware, 2004, p. 309, View Record in Scopus | Cited By in Scopus (1).
[8] H. Herr, R.D. Kornbluh, in: Y. Bar-Cohen (Ed.), Proceedings of the SPIE, vol. 5385, 2004, p. 1.
[9] Y. Bar-Cohen, in: Y. Bar-Cohen (Ed.), Proceedings of the SPIE, vol. 6168, 2006, p. 21.
[10] Y. Bar-Cohen, Electroacti®e Polymer(EAP)Actuators as Artificial Muscles — Reality, Potential and Challenges, SPIE Press, Washington, 2001.
[11] R.E. Pelrine, R.D. Kornbluh, J.P. Joseph, Sens. Actuators, A, Phys. vol. 64 (1998) 77.
[12] R. Heydt, R. Kornbluh, R. Pelrine, V. Mason, J. Sound Vib. vol. 215 (1998) 297.
[13] R. Pelrine, R. Kornbluh, J. Joseph, R. Heydt, Q. Pei, S. Chiba, Mater. Sci. Eng., C 11 (2000) 89.
[14] R. Pelrine, R. Kornbluh, Q. Pei, J. Joseph, Science 287 (2000) 836.
[15] R. Pelrine, R. Kornbluh, G. Kofod, Adv. Mater. 12 (2000) 1223.
[16] Q. Pei, R. Pelrine, S. Stanford, R. Kornbluh, M. Rosenthal, Symth. Met. 135–136 (2003) 129.
[17] G. Kofod, P. Sommer-Larsen, R. Kornbluh, R. Pelrine, J. Intell. Mater. Syst. Struct. 14 (2003) 787.
[18] F. Carpi, P. Chiarelli, A. Mazzoldi, D. De Rossi, Sens. Actuators, A, Phys. 107 (2003) 85.
[19] S. Ashley, Sci. Am. 10 (2003) 52.
[20] F. Carpi, D. De Rossi, Mater. Sci. Eng., C 24 (2004) 555.
[21] Y. Bar-Cohen, Proceedings of SPIE — The International Society for Optical Engineering, vol. 4695, 2002, p. 1.
[22] D. Pede, G. Serra, D. De Rossi, Mater. Sci. Eng., C 5 (1998) 289.
[23] S.C. Chang, J. Bharathan, Y. Yang, R. Helgeson, F. Wudl, M.B. Ramey, J.R. Reynolds, Appl. Phys. Lett. 73 (1998) 2561.
[24] T. Hebner, C.C. Wu, D. Marcy, M.H. Lu, J.C. Sturm, Appl. Phys. Lett. 72 (1998) 519.
[25] G.M. Whitesides, et al., Annu. Rev. Biomed. Eng. 3 (2001) 335.
[26] Z.N. Bao, J.A. Rogers, H.E. Katz, J. Mater. Chem. 9 (1999) 1895.
[27] T. Granlund, T. Nyberg, L.S. Roman, M. Svensson, O. Inganas, Adv. Mater. 12 (2000) 269.
[28] G. Vozzi, et al., Mater. Sci. Eng., C 20 (2002) 43.
[29] G. Vozzi, et al., Tissue Eng. 8 (2002) 1089.
[30] G. Vozzi, F. Carpi, A. Mazzoldi, Smart Mater. Struct. 15 (2006) 279.
[31] G. Vozzi, A. Previti, G. Ciaravella, A. Ahluwalia, J. Biomed. Mater. Res. 71A (2) (1 Nov 2004) 326.
[32] R.J. Stokes, D.F. Evans, Fundamentals of Interfacial Engineering, Wiley-VCH, New York, 1997.
[33] R.B. Martin, D.B. Burr, N.A. Sharkey, Skeletal Tissue Mechanics, Springer, 1998.